Available online at www.sciencedirect.com
SCIENCE DIRECT®
Solid State Sciences 7 (2005) 1096–1103
Solid State Sciences
www.elsevier.com/locate/ssscie

Metal-organic frameworks based on iron oxide octahedral chains connected by benzenedicarboxylate dianions

Tabatha R. Whitfield, Xiqu Wang *, Lumei Liu, Allan J. Jacobson *

Department of Chemistry and Center for Materials Chemistry, University of Houston, Houston, TX 77204-5003, USA

Received 12 December 2004; accepted 25 March 2005

Available online 15 June 2005

Abstract

Three new iron benzenedicarboxylates have been synthesized by solvothermal techniques, and their structures determined from single crystal X-ray data: $Fe(OH)(BDC)(py)_{0.85}$ (**1**), Fe(BDC)(DMF) (**2**), and $Fe(BDC)(py)_{0.42}(DMF)_{0.25}$ (**3**) (BDC = 1,4-benzenedicarboxylate, py = pyridine, DMF = *N*,*N*-dimethylformamide). Compounds **1** and **2** are the Fe(III)- and Fe(II)-structural analogs of the known Cr benzenedicarboxylate compound (MIL-53). Both contain *trans* corner-sharing FeO_6 octahedral chains connected by benzenedicarboxylate dianions. Compound **3** contains chains of iron oxygen octahedra that share both corners and edges. Each chain is linked by BDC to six other chains to form a three-dimensional framework. Crystal data: **1**, space group $I2/a$, $a = 6.889(2)$, $b = 11.073(3)$, $c = 18.280(6)$ Å, $\beta = 92.6(1)°$; **2**, space group $Pn2_1a$, $a = 19.422(2)$, $b = 7.3022(5)$, $c = 8.8468(7)$ Å; **3**, space group $P2_1/n$, $a = 9.234(2)$, $b = 17.243(3)$, $c = 9.978(2)$ Å, $\beta = 93.9(1)°$.

1. Introduction

Nanoporous hybrid inorganic/organic crystalline materials have attracted increasing interest due to their rich structural chemistry and tunable physical properties [1–8]. These hybrid frameworks, sometimes referred to as MOFs, can often be considered as expanded versions of typical inorganic structures where organic components act as linkers to connect inorganic clusters, chains or layers. A particularly well studied bridging organic component is the dianion of 1,4-benzenedicarboxylic acid and many compounds with very high porosity and variable pore sizes have been synthesized by using this ligand to connect together transition metal oxide clusters [9–11].

Recently, a group of hybrid compounds based on *trans* corner-sharing octahedral MO_6 chains were reported [12–17]. The metal oxide chains in these compounds are parallel to each other and are cross-linked by 1,4-benzenedicarboxylate (BDC) anions to form a framework with an array of channels. The first examples of the group were reported for the metals vanadium [12,13], chromium [14] and aluminum [16] by Férey and coworkers. The framework composition is $MOH{\cdot}BDC$ for $M = V^{3+}$, Cr^{3+}, Al^{3+} and $MO{\cdot}BDC$ for $M = V^{4+}$. In the trivalent metal structures, the OH occupies the shared position between adjacent octahedra along the chain. As synthesized, the compounds contain guest BDC molecules inside the channels that can be removed by heating. Once the channels are empty, other species may be intercalated. The structure is flexible so that on intercalation and deintercalation it expands and contracts to accommodate the specific guest molecule. This effect referred to by Férey and coworkers as "framework breathing" has been studied in some detail. The porous frameworks have good thermal stability (up to 500 °C) and can absorb small molecules such as hydrogen [15–17].

In our studies of this class of MOFs, we have reported an example in which 28% vanadium(III) is substituted by iron(III) [18]. Synthesis of the iron(III) phase is challenging because of the difficulty of avoiding the formation of iron oxide and/or reduction to Fe^{2+}. Here we re-

* Corresponding authors. Tel.: +1 713 7432785; Fax: +1 713 7432787.
E-mail addresses: xiqu.wang@mail.uh.edu (X. Wang), ajjacob@uh.edu (A.J. Jacobson).

1293-2558/$ – see front matter © 2005 Elsevier SAS. All rights reserved.
doi:10.1016/j.solidstatesciences.2005.03.007

port the synthesis and structures of three new iron BDC compounds Fe(OH)(BDC)(py)$_{0.85}$ (**1**), Fe(BDC)(DMF) (**2**), and Fe(BDC)(Py)$_{0.42}$(DMF)$_{0.25}$ (**3**) (py = pyridine, DMF = *N*,*N*-dimethylformamide). Compound **1** is the Fe^{3+} analog of the V^{3+}, Cr^{3+}, Al^{3+} compounds previously reported by Férey et al., **2** is to our knowledge the first example of a M^{2+} analog where the bridging species along the chain is neutral, and **3** is a more complex structure in which pyridine molecules are also coordinated to iron atoms.

2. Experimental section

2.1. Materials and methods

All starting materials were reagent grade and were used as purchased. The synthesis products were examined with a polarizing optical microscope and a JEOL-JSM6400 scanning electron microscope with a Link Analytical EXL spectrometer for EDX analysis. Infrared spectra were collected with a Galaxy FTIR 5000 spectrometer using the KBr pellet method.

2.2. Synthesis of Fe(OH)(BDC)(py)$_{0.85}$ (1)

In a typical synthesis of **1**, a mixture of $Fe(NO_3)_3{\cdot}9H_2O$ (Alfa, 0.404 g, 1 mmol), H_2BDC (Aldrich, 0.170 g, 1 mmol), H_2O_2 (Aldrich, 0.25 ml), pyridine (Aldrich, 0.5 ml) and DMF (EM Science, 10 ml) was sealed in a Parr autoclave with a 23 ml Teflon liner in air. The mixture was subsequently heated to 180 °C at a rate of 1 °C/min and allowed to react for 2 d. The autoclave was then cooled to 30 °C at a rate of 0.5 °C/min. The final product was filtered and washed with DMF. Yellow needles of compound **1** were present as a minor phase (∼ 5%). The major phase in the product was an amorphous orange powder. Extensive intergrowth between the tiny needles and the impurities makes it extremely difficult to manually separate them. EDX analysis gave the Fe content of 19.1% consistent with the calculated value of 18.24% from the formula derived from crystal structure refinements.

2.3. Synthesis of Fe(BDC)(DMF) (2)

Compound **2** was similarly synthesized from a mixture of FeOOH (Aldrich, 0.088 g, 1 mmol), H_2BDC (Aldrich, 0.170 g, 1 mmol), and DMF (EM Science, 10 ml). The mixture was sealed in a Parr autoclave with a 23 ml Teflon liner in air, and heated at 180 °C for 2 d. The autoclave was then cooled to room temperature in air over ∼ 4 h. The final product was filtered and washed with DMF. Orange polyhedral crystals of **2** were recovered together with unreacted FeOOH. The yield was ∼ 15% based on iron. EDX analysis: found Fe 20.2%, calculated: 19.06%. Infrared spectrum (cm^{-1}): 540(s), 750(s), 815(m), 886(w), 1017(m), 1113(w), 1152(m), 1386(vs), 1504(s), 1567(vs), 3192(br), 3340(br).

2.4. Synthesis of Fe(BDC)(py)$_{0.42}$(DMF)$_{0.25}$ (3)

In a typical synthesis of **3**, a mixture of FeOOH (Aldrich, 0.088 g, 1 mmol), H_2BDC (Aldrich, 0.170 g, 1 mmol), pyridine (Aldrich, 0.5 ml) and DMF (EM Science, 10 ml) was sealed in a Parr autoclave with a 23 ml Teflon liner in air, and heated at 180 °C for 2 d. The autoclave was then cooled to room temperature in air over ∼ 4 h. Brown polyhedral crystals of **3** were recovered together with unreacted FeOOH. The yield was ∼ 20% based on iron. EDX analysis: found Fe 21.1%, calculated 20.59%. Infrared spectrum (cm^{-1}): 434(w), 448(w), 524(s), 630(m), 688(m), 702(s), 749(vs), 810(m), 827(m), 849(m), 881(w), 1017(m), 1072(w), 1109(w), 1150(w), 1219(w), 1260(w), 1325(m), 1364(vs), 1392(s), 1406(s), 1448(m), 1506(m), 1560(s), 1602(vs), 1670(s), 2991(w), 3067(w), 3260(w), 3448(br).

2.5. X-ray crystallography

For crystal structure determination, single crystal X-ray diffraction data were measured on a SMART platform diffractometer equipped with a 1 K CCD area detector using graphite-monochromatized MoK_α radiation at 293 K. A hemisphere of data (1271 frames at 5 cm detector distance) was collected for each phase using a narrow-frame method with scan widths of 0.30° in ω and an exposure time of 30–50 s/frame. The first 50 frames were remeasured at the end of data collection to monitor instrument and crystal stability. The data were integrated using the Siemens SAINT program, with the intensities corrected for Lorentz factor, polarization, air absorption, and absorption due to variation in the path length through the detector faceplate [19]. Absorption corrections were made using the program SADABS [20]. The structures were solved and refined using SHELXTL [21]. The hydrogen atoms were refined with geometrical constraints. The *R* values for **1** are slightly higher than normal because of the small crystal size. The thermal parameters for atoms of the pyridine guest molecules in **1** are relatively large because of the fractional occupancy. Crystallographic and refinement details are summarized in Table 1. Refined atomic coordinates are listed in Tables 2–4.

3. Results and discussion

3.1. Synthesis and characterization

All three new compounds were synthesized in the form of single crystals suitable for detailed structure studies. Despite many variations in the synthesis conditions, however, all three phases were obtained as minor phases with low yield. Because of the ease of hydrolysis of Fe(III) ions, water was removed from the reactants in order to try to optimize the synthesis of compound **1**. Approaches such as drying the DMF solvent with molecular sieves, replacing H_2O_2 with metal peroxides and substitution of $Fe(NO_3)_3{\cdot}9H_2O$

Table 1
Crystal data and structure refinement details

	1	**2**	**3**
Formula	$C_{12.25}H_{9.25}FeN_{0.85}O_5$	$C_{11}H_{11}FeNO_5$	$C_{10.85}H_{7.85}FeN_{0.67}O_{4.25}$
F.W.	304.21	293.06	271.46
Temperature / K	293(2)	293(2)	293(2)
Space group	$I2/a$	$Pn2_1a$	$P2_1/n$
a / Å	6.889(2)	19.422(2)	9.234(2)
b / Å	11.073(3)	7.3022(5)	17.243(3)
c / Å	18.280(6)	8.8468(7)	9.978(2)
β / °	92.6(1)	90	93.9(1)
V / Å^3	1392.9(7)	1254.7(2)	1584.9(5)
Crystal size / mm^3	0.10 × 0.02 × 0.02	0.42 × 0.36 × 0.26	0.16 × 0.12 × 0.09
Refl. collected / unique	3661 / 1580	7422 / 2793	9454 / 3600
R_{int}	0.1886	0.0439	0.0343
Data / parameters	1580 / 96	2793 / 152	3600 / 241
Goodness-of-fit	0.941	1.057	1.070
$R1$ / $wR2(I > 2\sigma(I))$	0.0856 / 0.1456	0.0350 / 0.1038	0.0440 / 0.1159
$R1$ / $wR2$ (all data)	0.2188 / 0.1852	0.0530 / 0.1141	0.0572 / 0.1221

$R1 = \sum ||F_o| - |F_c|| / \sum |F_o|$, $wR2 = [\sum(w(F_o^2 - F_c^2)^2) / \sum(wF_o^2)^2]^{1/2}$.

Table 2
Atomic coordinates ($\times 10^4$) and equivalent isotropic displacement parameters (Å$^2 \times 10^3$) for Fe(OH)(BDC)(py)$_{0.85}$ (**1**)

	x	y	z	U_{eq}
Fe(1)	0	0	0	15(1)
O(1)	7500	818(7)	0	23(2)
O(2)	1103(7)	1260(5)	712(3)	26(1)
O(3)	−675(7)	−1006(5)	888(3)	27(1)
C(1)	2596(11)	1946(8)	1815(4)	33(2)
C(2)	4262(11)	2157(9)	2252(5)	45(3)
C(3)	2650(12)	1340(7)	1085(4)	29(2)
C(4)	825(11)	2295(9)	2085(5)	46(3)
C(5)	7500	5870(40)	0	340(60)
C(6)	7890(60)	5140(20)	−594(16)	260(20)
C(7)	7980(40)	3880(20)	−535(14)	156(11)
N(1)	7500	3242(17)	0	143(13)

U_{eq} is defined as one third of the trace of the orthogonalized U_{ij} tensor.

Table 3
Atomic coordinates ($\times 10^4$) and equivalent isotropic displacement parameters (Å$^2 \times 10^3$) for Fe(BDC)(DMF) (**2**)

	x	y	z	U_{eq}
Fe(1)	5001(1)	4693(6)	4999(1)	18(1)
O(1)	5845(2)	5669(4)	6162(5)	33(1)
O(2)	4179(2)	3721(4)	3757(5)	34(1)
O(3)	4252(2)	5654(4)	6518(5)	34(1)
O(4)	5734(2)	3707(4)	3454(5)	35(1)
O(5)	5047(1)	2160(10)	6400(2)	28(1)
C(1)	6112(1)	7158(12)	6376(3)	24(1)
C(2)	6861(1)	7233(8)	6872(2)	27(1)
C(3)	7204(2)	8881(7)	7100(6)	50(2)
C(4)	7889(2)	8880(8)	7554(6)	45(2)
C(5)	8231(1)	7232(9)	7781(2)	27(1)
C(6)	7888(2)	5583(8)	7553(7)	48(2)
C(7)	7203(2)	5584(7)	7098(7)	45(2)
C(8)	3979(1)	7144(11)	6709(3)	26(1)
C(9)	4760(2)	2187(15)	7670(3)	38(1)
C(10)	5812(2)	2279(16)	9021(5)	82(2)
C(11)	4713(3)	2072(15)	10415(5)	83(2)
N(1)	5065(1)	2267(15)	8958(3)	40(1)

U_{eq} is defined as one third of the trace of the orthogonalized U_{ij} tensor.

Table 4
Atomic coordinates ($\times 10^4$) and equivalent isotropic displacement parameters ($Å^2 \times 10^3$) for $Fe(BDC)(py)_{0.42}(DMF)_{0.25}$ (**3**)

	x	y	z	U_{eq}
Fe(1)	8741(1)	236(1)	1059(1)	16(1)
Fe(2)	5000	0	0	19(1)
O(1)	10999(2)	437(1)	743(2)	20(1)
O(2)	8095(2)	1226(1)	56(2)	23(1)
O(3)	13392(2)	505(1)	1196(2)	25(1)
O(4)	5704(2)	1107(1)	−489(2)	24(1)
O(5)	6571(2)	−39(1)	1697(2)	20(1)
O(6)	8025(3)	657(1)	3047(2)	27(1)
C(1)	6885(3)	274(2)	2839(3)	19(1)
C(2)	5893(3)	137(2)	3952(3)	19(1)
C(3)	4791(4)	−410(2)	3801(3)	22(1)
C(4)	6111(4)	545(2)	5163(3)	22(1)
C(5)	6895(3)	1452(2)	−498(3)	19(1)
C(6)	6906(4)	2212(2)	−1249(3)	22(1)
C(7)	8051(4)	2730(2)	−1032(4)	37(1)
C(8)	8080(4)	3412(2)	−1767(4)	36(1)
C(9)	5761(4)	2408(2)	−2159(4)	26(1)
C(10)	12133(3)	728(2)	1360(3)	17(1)
C(11)	6973(3)	3585(2)	−2729(3)	20(1)
C(12)	5785(4)	3091(2)	−2897(3)	24(1)
N(1P)	9195(6)	−868(2)	2156(4)	35(2)
C(1P)	10144(5)	−878(3)	3299(5)	45(2)
C(2P)	10390(6)	−1566(3)	4007(5)	68(3)
C(3P)	9687(7)	−2242(3)	3571(6)	70(3)
C(4P)	8738(7)	−2231(3)	2429(6)	62(2)
C(5P)	8492(6)	−1544(3)	1721(5)	53(3)
O(1D)	9572(11)	−754(6)	2117(10)	27(2)
N(1D)	9223(13)	−1950(7)	2715(12)	49(3)
C(1D)	8782(17)	−1401(9)	2031(14)	34(3)
C(2D)	10360(30)	−1936(14)	3710(20)	78(7)
C(3D)	8445(19)	−2686(10)	2422(18)	68(5)

U_{eq} is defined as one third of the trace of the orthogonalized U_{ij} tensor.

by FeOOH, $FeCl_3$ or $Fe_2(SO_4)_3$ did not improve the yield. Experiments with various reactant ratios were carried out, but no satisfactory high yield synthesis has yet been developed for any of the three new compounds. Nevertheless, the compounds can be obtained reproducibly and represent an extension of this interesting class of structures.

The IR spectrum of **2** exhibits characteristic bands of BDC at 1567 cm^{-1} for the antisymmetric stretching vibrations and at 1386 cm^{-1} for the symmetric ones of the carboxyl groups. Their separation of 181 cm^{-1} is in the usual range for bridging carboxyl groups [22]. The band at 1504 cm^{-1} is typical for DMF with the oxygen atom coordinated to a metal atom. The IR spectrum of compound **3** shows highly complicated features due to the random substitution of coordinated DMF for pyridine. The bands in the ranges 1602–1560 and 1406–1364 cm^{-1} may be attributed to the bridging and chelating carboxyl groups. The band at 1506 cm^{-1} is in the typical range for coordinating DMF. The band at 630 cm^{-1} is characteristic for coordinating pyridine ligands (in-plane ring deformation) [22].

3.2. Crystal structure of *1*

The 3-dimensional framework of **1** is closely similar to those of the previously reported V(III) MIL-47, and Cr(III), Al(III) MIL-53 compounds (Fig. 1). In **1**, the iron oxygen octahedron is slightly compressed with an axial Fe–O bond length of 1.946(5) Å and equatorial Fe–O bond lengths of 2.031(5)–2.041(5) Å. The axial oxygen atoms are shared by neighboring octahedra to form a zigzag …OH–Fe–OH–Fe–… backbone with a Fe–OH–Fe angle of 124.5(4)°. The equatorial oxygen atoms are shared with the dicarboxylate anions that cross-link the octahedral chains into a 3D framework. The framework may be considered as a laterally expanded ReO_3 structure. Bond valence sums calculated for the Fe and the axial oxygen atoms are 3.10 and 1.25 v.u., in agreement with their assignment as Fe(III) and OH ions, respectively [23]. The rhomb-shaped channels of the framework are filled by pyridine molecules. Neighboring pyridine molecules are parallel to each other but have opposite orientations. Each pyridine molecule is hydrogen bonded to an OH group of the octahedral chain with the N···O distance of 2.68(2) Å. The N···C axis of the pyridine ring is perpendicular to the octahedral chains (Fig. 1(a)). The angle between the pyridine ring and the octahedral chain is 73°. The orientation of the pyridine ring is probably a result of a compromise between geometric requirements of the N···H–O hydrogen bonds and π–π interactions between neighboring pyridine rings (ring···ring distance: 3.27 Å)

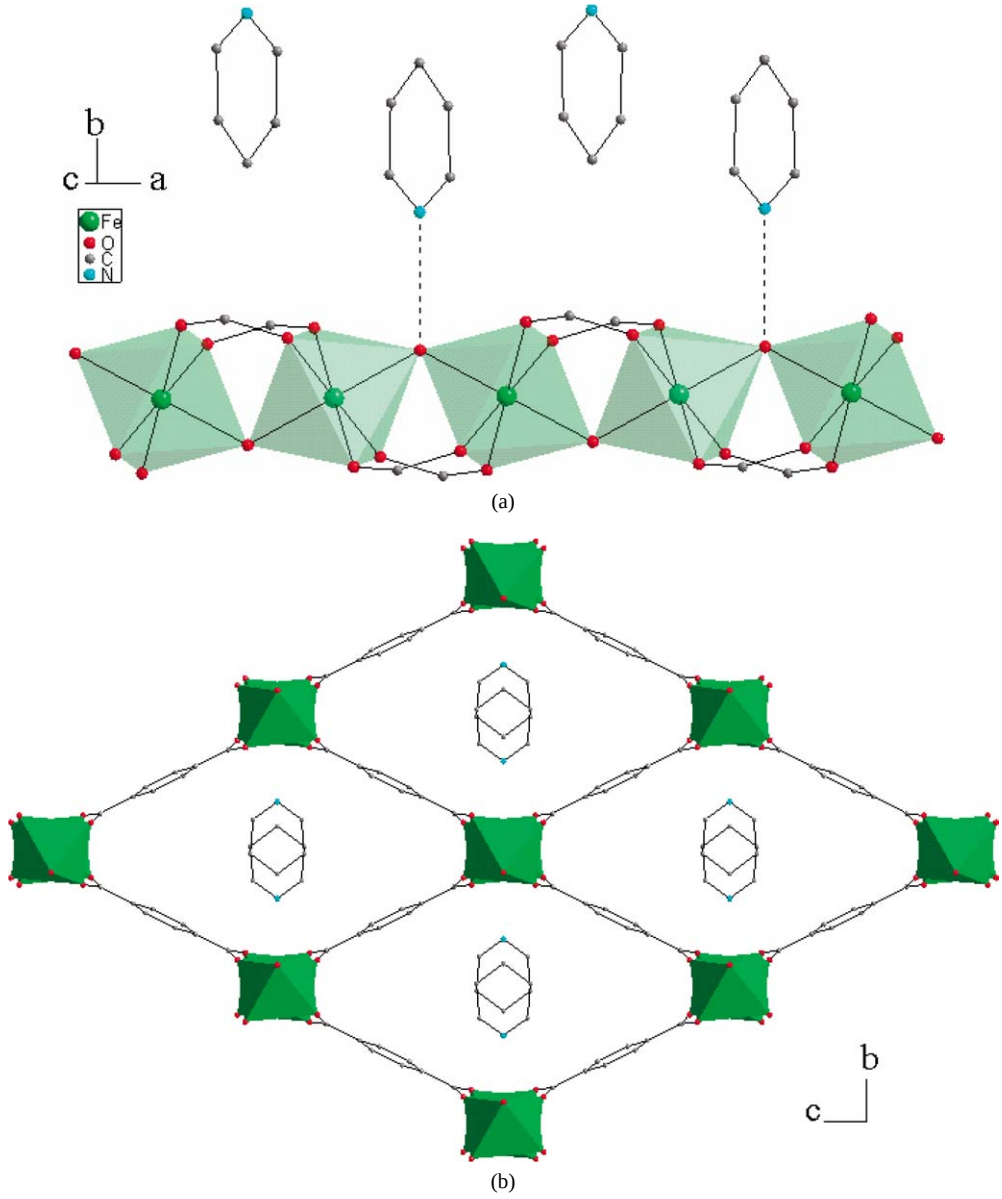

Fig. 1. (a) The octahedral chain and the pyridine molecules in **1**. The dashed lines represent hydrogen bonds. (b) A projection of the structure of **1** along [100].

[24]. Crystal structure refinements indicate that the pyridine sites are not fully occupied. The refined occupancy corresponds to 0.85(2) pyridine molecule per Fe atom. The incomplete occupancy may be a consequence of pyridine loss on exposure to atmosphere or it may be due to defects (missing pyridine molecules) that are needed to match the pyridine lattice repeat to that of the Fe–OH–Fe chain.

*3.3. Crystal structure of **2***

Compound **2** has a structure related to that of compound **1** (Fig. 2). In contrast to the compressed FeO_6 octahedra in **1**, the iron oxygen octahedra in **2** are elongated with the axial Fe–O bond lengths of 2.188(6)–2.228(6) Å and equatorial bond lengths of 2.062(4)–2.103(4) Å. The bond valence sum calculated for the Fe atom is 2.12 v.u., consistent with Fe(II). The axial oxygen atom is shared by two octahedra and a DMF molecule (Fig. 2(a)). The planar DMF molecule is perpendicular to the octahedral chain (Fig. 2(b)). The Fe–O–Fe angle in the octahedral chain of **2** is 111.5(1)°, considerably smaller than the corresponding angle 124.5(4)° in **1**. The Fe···Fe distance in **2** (3.651(1) Å), however, is longer than in **1** (3.444(1) Å) because of the long axial Fe–O bonds in the former.

A significant difference between the frameworks of **2** and **1** is in the opening of the rhombus-shaped channels. The acute angle of the rhombus outlined by the octahedral chains is a measure of the opening of the channels. This angle is 54.4° in **2**, compared with 69.3° in **1** because of the larger channel opening in the latter. Table 5 lists the correspond-

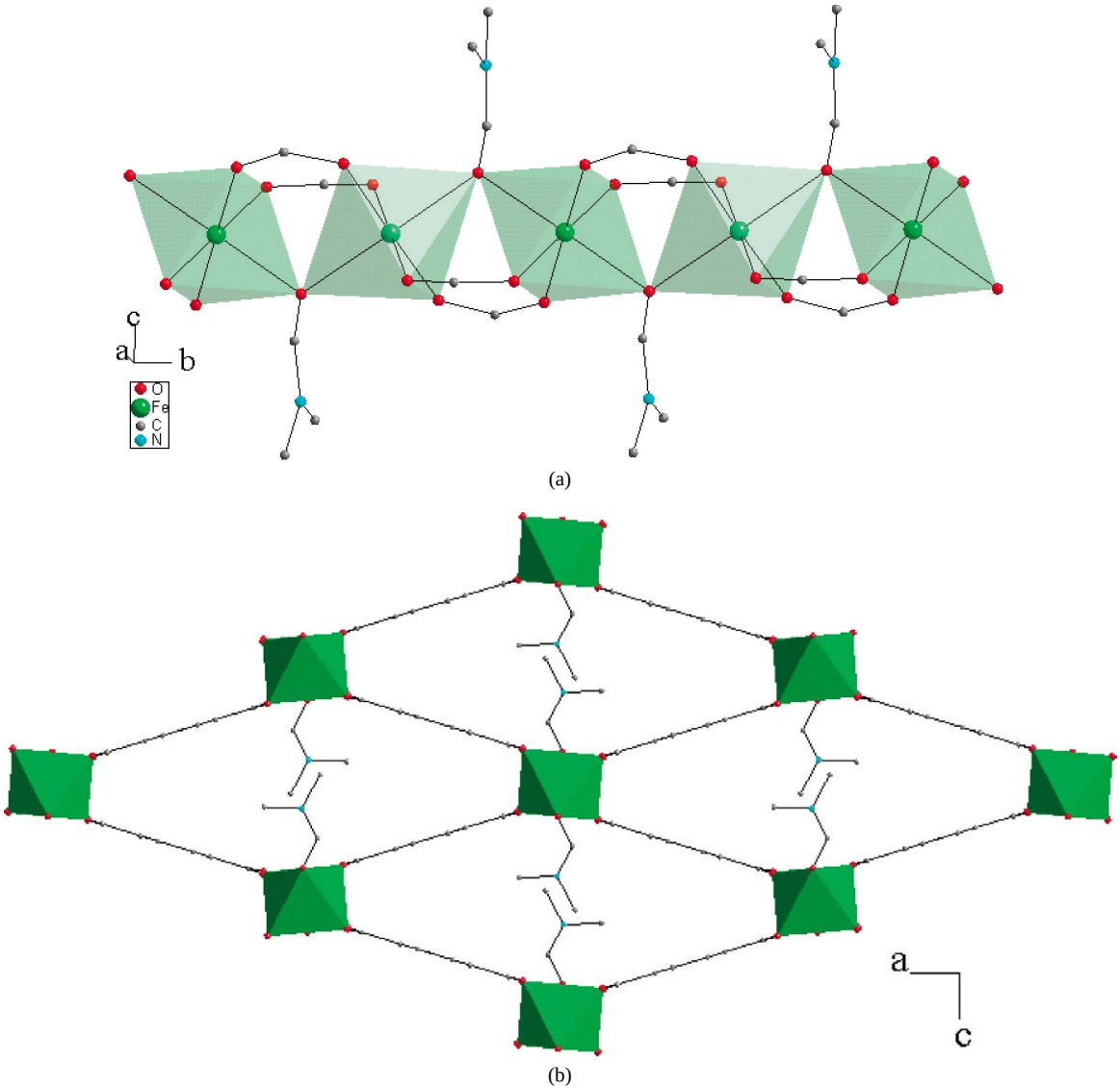

Fig. 2. (a) The octahedral chain in **2**. (b) A projection of the structure of **2** along [010].

ing angles in the Cr(III) and Al(III) phases with the MIL-53 structures [15,17]. The calcined phases with empty channels have the largest channel openings. When the channels are filled by guest species, the channel opening decreases because of the interactions between the frameworks and the guest molecules. In the case of the hydrated phases, hydrogen bonds between water molecules inside the channels and oxygen atoms of the framework BDC are responsible for the large change in the channel openings. The channel opening of compound **1** is comparable to the Cr(III) phase with absorbed DMF guest molecules that are not covalently bonded to the framework, probably because of the similar sizes of the DMF and pyridine guest molecules and similar hydrogen bonds between the guest molecules and the octahedral chains. The channel opening of compound **2** is between those of **1** and the hydrated phases. The oxygen atom of DMF in **2** is directly bonded to the Fe atoms of the octahedral chains. The other atoms of DMF in **2** have van der Waals interactions or extremely weak C–H···O hydrogen bond interactions with the framework [25].

3.4. Crystal structure of 3

Compound **3** has a new 3-dimensional structure (Fig. 3). There are two different Fe sites. The Fe1 octahedron has five oxygen atom corners shared with BDC, two of which are chelating and the other three bridging. The sixth corner is either a nitrogen atom from a pyridine molecule or an oxygen atom from a DMF molecule. The Fe2 octahedron has six oxygen atom corners all shared with BDC and all are bridging. The Fe–O bond lengths are in the range of 2.046(2)–2.254(2) Å and the Fe–N bond length is 2.222(3) Å. Bond valence sums calculated for Fe1 and Fe2 are 1.94 and 2.07 v.u., respectively, consistent with Fe^{2+}. Two Fe1 octahedra

Table 5
The acute angle of the rhombus-shaped channel sections and guest molecules in different phases with the MIL-53 framework topology

Framework cation	Cr(III) [15]	Al(III) [17]	Fe(III)	Fe(II)
As synthesized	78.0° / BDC	78.7° / BDC	69.3° / pyridine	54.4° / DMF
Calcined	83.9° / –	83.4° / –		
Absorption of DMF	71.3° / DMF			
Absorption of water	48.3° / H_2O	47.4° / H_2O		

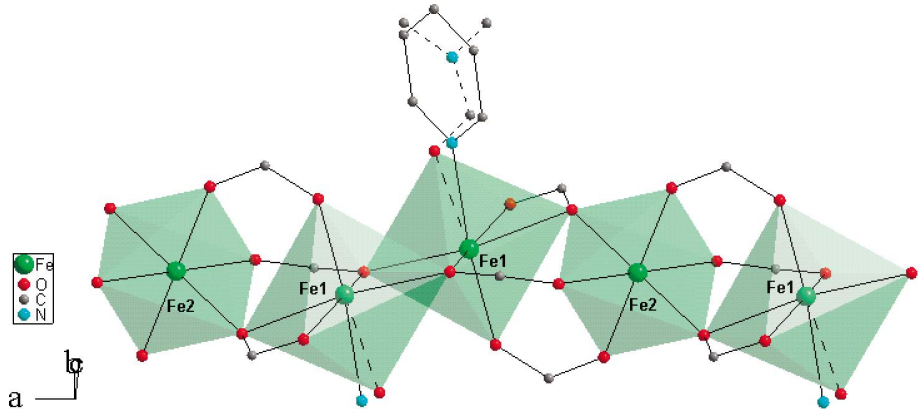

(a)

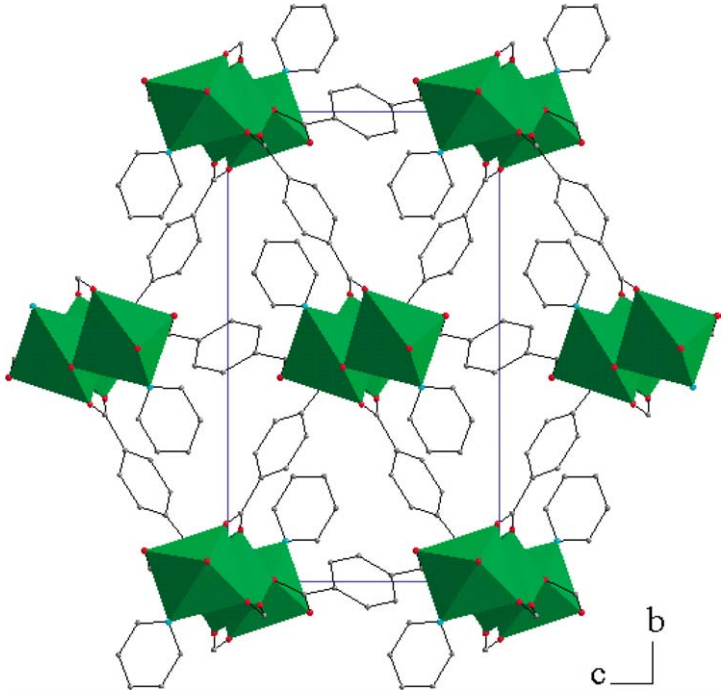

(b)

Fig. 3. (a) The octahedral chain in **3**. The DMF molecules substituting for pyridine are marked by dashed lines. (b) A projection of the structure of **3** along [100]. The DMF are omitted.

share a common edge to form a dimer with an inversion center. The dimers are alternatively connected by the Fe2 octahedra to form 1-dimensional chains (Fig. 3(a)). Each Fe2 octahedron shares two *trans* corners with two Fe1 dimers. Each octahedral chain is cross-linked to six other chains by BDC to form the 3-dimensional structure (Fig. 3(b)). The pyridine molecules are oriented to point into the triangular channels of the framework structure, and are partially substituted by DMF molecules (Fig. 3). The pyridine/DMF ratio was refined to 0.42/0.25(1) from the single crystal X-ray data.

4. Conclusions

The Fe(III) analog (**1**) of the M(OH)·BDC, M =V, Cr, Al phases (MIL-47 and MIL-53) has been synthesized in

single crystal form. As synthesized, the channels in **1** are filled by pyridine molecules instead of H_2BDC molecules that are found in the channels of all other as-synthesized MIL-47 and MIL-53 phases. The pyridine molecules are oriented so that the rings are perpendicular to the channel and are weakly hydrogen bonded to the bridging hydroxyl ions. The Fe(II) analog FeDMF·BDC(**2**) that has been obtained also in single crystal form, is the first divalent metal example of this structure type. In **2**, the oxygen atom from the DMF molecule is the bridging atom along the octahedral chain. The sequence of compositions M(II)OCN$(CH_3)_2$·BDC, M(III)OH·BDC, M(IV)O·BDC is analogous to that observed in vanadium phosphate structures that are based on trans connected distorted octahedral chains. Thus in the series V(III)H_2O·PO_4, V(IV)OH·PO_4 and V(V)O·PO_4, the oxidation state of vanadium in the three closely related structures, changes as the bridging ligand changes from a neutral water molecule to a hydroxide and finally to an oxide ion [26,27]. In the vanadium phosphates, the compounds are inter-convertible and consequently the oxidation of V(III)OH·BDC to V(IV)O·BDC observed by Férey on oxidative removal of the template is not unexpected. Intermediate oxidation states also appear to be a possibility.

The MO_6 octahedral chains in the MOBDC series, are isolated from each other by the bridging BDC ligands resulting in the generation of one-dimensionally confined atomic M–O–M–O–M 'wires' which are expected to have unusual optical and electronic properties. Indeed, the titanosilicate ETS-10 with a band gap of about 4 eV which contains similar Ti–O–Ti–O–Ti–O chains isolated by silicate anions has been studied from this perspective as a model system [28].

Compound **3** exhibits a new type of octahedral chain, which is cross-linked by BDC to six neighboring chains. A similar cross-linking pattern of octahedral chains is also found in the recently reported Fe(III) dicarboxylate MIL-85 in which the octahedral chains are decorated by bridging acetate groups [29]. Recently, the corner-sharing octahedral chains in the MIL-47 structures have been linked by BDC to form frameworks (MIL-68) with an expanded hexagonal bronze topology [30]. Given the variations in the octahedral chain geometries and in the linking patterns adopted by BDC, more novel phases with different channel shapes are anticipated.

Supplementary material

The supplementary material has been sent to the Cambridge Crystallographic Data Centre, 12 Union Road, Cambridge CB2 1EZ, UK, as supplementary material CCDC-258444, CCDC-258445 and CCDC-258446, and can be obtained by contacting the CCDC (quoting the article details and the corresponding CCDC number).

Acknowledgements

We thank the National Science Foundation (DMR-0120463), the R.A. Welch Foundation for financial support. This work made use of Shared Experimental Facilities of the Center for Materials Chemistry (CMC-UH) at the University of Houston.

References

[1] C. Robl, Mater. Res. Bull. 27 (1992) 99.
[2] A. Clearfield, Curr. Opin. Solid State Mater. Sci. 1 (1996) 268.
[3] M. Zaworotko, Nature 386 (1997) 220.
[4] C. Janiak, Angew. Chem. Int. Ed. Engl. 36 (1997) 1431.
[5] S. Feng, R. Xu, Acc. Chem. Res. 34 (2001) 239.
[6] G. Férey, Chem. Mater. 13 (2001) 3084.
[7] O.M. Yaghi, M. O'Keeffe, N.W. Ockwig, H.K. Chae, M. Eddaoudi, J. Kim, Nature 423 (2003) 705.
[8] S. Kitagawa, R. Kitaura, S. Noro, Angew. Chem. Int. Ed. Engl. 43 (2004) 2334.
[9] M. Eddaoudi, D.B. Moler, H. Li, B. Chen, T. Reineke, M. O'Keeffe, O.M. Yaghi, Acc. Chem. Res. 34 (2001) 319.
[10] N.L. Rosi, J. Eckert, M. Eddaoudi, D.T. Vodak, J. Kim, M. O'Keeffe, O.M. Yaghi, Science 300 (2003) 1127.
[11] H.K. Chae, D.Y. Siberio, J. Kim, Y. Go, M. Eddaoudi, A.J. Matzger, M. O'Keeffe, O.M. Yaghi, Nature 427 (2004) 523.
[12] K. Barthelet, D. Riou, G. Férey, Chem. Commun. (2002) 1492.
[13] K. Barthelet, J. Marrot, D. Riou, G. Férey, Angew. Chem. Int. Ed. Engl. 41 (2002) 281.
[14] F. Millange, C. Serre, G. Férey, Chem. Commun. (2002) 822.
[15] C. Serre, F. Millange, C. Thouvenot, M. Nogues, G. Marsolier, D. Louër, G. Férey, J. Am. Chem. Soc. 124 (2002) 13519.
[16] G. Férey, M. Latroche, C. Serre, F. Millange, T. Loiseau, A. Percheron-Guégan, Chem. Commun. (2003) 2976.
[17] T. Loiseau, C. Serre, C. Huguenard, G. Fink, F. Taulelle, M. Henry, T. Bataille, G. Férey, Chem.-Eur. J. 10 (2004) 1373.
[18] T.R. Whitfield, X. Wang, A.J. Jacobson, Mat. Res. Soc. Symp. Proc. 755 (2003) 191.
[19] SAINT, Program for Data Extraction and Reduction, Siemens Analytical X-Ray Instruments Inc., Madison, USA, 1996.
[20] G.M. Sheldrick, SADABS, Program for Siemens Area Detector Absorption Corrections, University of Gottingen, Germany, 1997.
[21] G.M. Sheldrick, SHELXTL, Program for Refinement of Crystal Structures, Siemens Analytical X-Ray Instruments Inc., Madison, USA, 1994.
[22] K. Nakamoto, Infrared and Raman Spectra of Inorganic and Coordination Compounds, John Wiley, New York, 1986.
[23] N.E. Brese, M. O'Keeffe, Acta Crystallogr. B 47 (1991) 192.
[24] C. Janiak, Dalton Trans. (2000) 3885.
[25] G.R. Desiraju, T. Steiner, The Weak Hydrogen Bond in Structural Chemistry and Bology, Oxford Univ. Press, Oxford, 1999.
[26] J.T. Vaughey, W.T.A. Harrison, A.J. Jacobson, D.P. Goshorn, J.W. Johnson, Inorg. Chem. 33 (1994) 2481.
[27] S.C. Lim, J.T. Vaughey, W.T.A. Harrison, L.L. Dussack, A.J. Jacobson, Solid State Ionics 84 (1996) 219.
[28] A. Damin, F.X. Llabres i Xamena, C. Lamberti, B. Civalleri, C.M. Zicovich-Wilson, A. Zecchina, J. Phys. Chem. B 108 (2004) 1328.
[29] C. Serre, F. Millange, S. Surble, J.-M. Greneche, G. Férey, Chem. Mater. 16 (2004) 2706.
[30] K. Barthelet, J. Marrot, G. Férey, D. Riou, Chem. Commun. (2004) 520.